



Low temperature dependence of electrical resistivity: Implications for near surface geophysical monitoring

Kevin Hayley,¹ L. R. Bentley,¹ M. Gharibi,¹ and M. Nightingale¹

Received 27 June 2007; revised 4 August 2007; accepted 17 August 2007; published 18 September 2007.

[1] Electrical resistivity imaging surveys are used to monitor variations in pore fluid chemistry and saturation as well as time-lapse changes. Temperature variations in the near surface can produce larger magnitude changes in electrical conductivity than changes due to slow moving solute plumes or spatial variations in chemistry and soil moisture. Relationships between temperature and electrical conductivity based on previous studies conducted over 25–200°C do not explain 0–25°C laboratory data. A modification to the temperature dependence within a petrophysical model is proposed that may allow general application over this temperature range. An empirical linear approximation of 1.8 to 2.2 percent change in bulk electrical conductivity per degree C is consistent with low temperature electrical conductivity studies and the predictions of the petrophysical model used. This relationship can be used to account for the effect of temperature variations within individual images or time-lapse difference images. **Citation:** Hayley, K., L. R. Bentley, M. Gharibi, and M. Nightingale (2007), Low temperature dependence of electrical resistivity: Implications for near surface geophysical monitoring, *Geophys. Res. Lett.*, *34*, L18402, doi:10.1029/2007GL031124.

1. Introduction

[2] The electrical conductivities of rocks and soils are highly dependent on water saturation and ionic concentration within the pore water. Variations in electrical conductivity (EC) are used in the time-lapse electrical resistivity imaging (ERI) studies to track tracer migration [e.g., *Daily et al.*, 1992; *Kemna et al.*, 2002; *Slater and Sandberg*, 2000] monitor infiltration [e.g., *Barker and Moore*, 1998; *Binley et al.*, 2002; *French and Binley*, 2004] and to monitor contaminate transport and remediation. *Hauck* [2002] used time-lapse ERI to monitor frozen ground and related the observed differences to changes in liquid water saturation and temperature.

[3] Temperature has a strong influence on the EC of the subsurface [*Sen and Goode*, 1992; *Waxman and Thomas*, 1974]. *Rein et al.* [2004] studied the effect of temperature, soil moisture, and temporal variation of the ambient ionic concentration on tracer tests, and concluded that even diurnal temperature variations can have a relatively large effect. Yet in most time-lapse studies, the influence of temperature variations has not been accounted for. Our purpose is to examine the near surface temperature dependence of electrical conductivity, establish a general temperature conductivity relationship, and implement a practical

framework to account for temperature effects in time-lapse electrical surveys.

2. Electrical Conduction in Rocks and Sediments: Theory and Models

[4] Electrical conduction in rocks and sediments occurs through conduction in the pore fluid and by surface conduction near the grain surface [*Revil et al.*, 1998; *Waxman and Smits*, 1968]. Petrophysical models can relate observed bulk EC to these mechanisms by considering them as parallel resistors [*Waxman and Smits*, 1968], or by effective medium theory. The effective medium theory is based on infinitely resistive matrix grains with a specific surface conductance immersed in a conductive medium [*Bussian*, 1983; *Revil et al.*, 1998]. Changes in the surface EC with temperature are due to changes in the surface ionic mobility, while changes in the fluid EC are primarily due to changes in the fluid viscosity. The temperature dependence of these two mechanisms is different. Two types of temperature dependence relationships have been proposed: linear and exponential. The exponential model [*Llera et al.*, 1990] has the form for normalized conductivity:

$$\sigma^T / \sigma^{25} = e^{\frac{-A}{R}(\frac{1}{T} - \frac{1}{298})} \quad (1)$$

where: A is the activation energy of conduction; R is the universal gas constant; T is the temperature in Kelvin; and σ^T and σ^{25} are the electrical conductivities at temperature T and 25°C respectively.

[5] The linear model is of the form:

$$\sigma^T / \sigma^{25} = m(T - 25) + 1 \quad (2)$$

[*Hayashi*, 2004; *Sen and Goode*, 1992], where σ^T and T are the recorded EC and temperature in degrees Celsius. σ^{25} is the electrical conductivity at the conventional reference temperature of 25°C and m is the fractional change in EC per degree Celsius.

3. Laboratory Experiment

[6] Laboratory experiments were conducted to examine the temperature EC relationship on samples from a site of a time-lapse ERI survey. Material at the site consists of a predominantly fine grained glacial till with sporadic pebbles and cobbles in the sandy clay matrix. Grain size analysis on samples gives mean values of 32% sand, 50% silt, and 18% clay. The average cation exchange capacity from the site was 20 meq/100 g with a range of 10–30 meq/100 g. The

¹Department of Geoscience, University of Calgary, Calgary, Alberta, Canada.

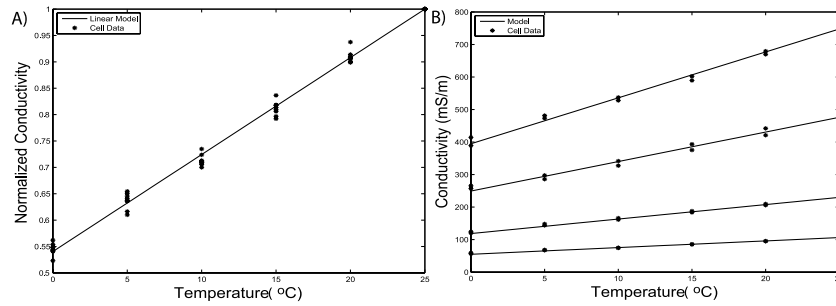


Figure 1. Bulk electrical conductivity as a function of temperature. (a) Normalized conductivity of the eight samples with a linear model fit (equation 2) using $m = 0.0183$. (b) EC vs. temperature for eight samples fit to the model by *Revil et al.* [1998] using $m^f = 0.0187$, $m^s = 0.018$, $B^{25} = 0.51 \text{ e-}08 \text{ m}^2/\text{sV}$.

average estimated porosity for the samples was 0.3. A subsurface brine plume is being monitored and remediated at this site and the pore fluid is NaCl dominated.

[7] The experimental apparatus for measuring the EC consisted of a cylindrical non conducting cell with copper plate electrodes at each end. A filter paper soaked with a 1 molar CuSO_4 solution was placed between the copper electrodes and the sample to assure good electrical contact and to minimize charge build up effects. The cell had an internal thermocouple and was placed in a precision temperature incubator set at the desired temperature for each reading. Four samples from direct push core representing different subsurface levels of salt concentration were homogenized, split and repacked in the cell in order to test repeatability resulting in eight measurements sequences. The samples were saturated and loaded using a loading device to simulate the effective stress on the samples at the in-situ depth. Resistance measurements were made with a Hewlett-Packard™ 4262A inductance-capacitance-resistance (LCR) meter following the method described by *Wong et al.* [2004]. The LCR meter measures resistance, capacitance and inductance at three test frequencies of 120 Hz, 1 kHz and 10 kHz. The 10 kHz measurement values are used, because they have minimal charge build up effects as evidenced by the low measured specific capacitance values (on the order of 10 nF/m). Resistance measurements were converted to resistivity using the geometric factor for a cylinder, and reported as EC.

[8] Figure 1a shows the bulk EC normalized by the respective 25°C measurement as a function of temperature for the four different samples and their duplicates. The normalized data is well described by the linear model in equation (2) for bulk EC with a best fit slope of $m = 0.0183$. The slopes are consistent across a large range of salt concentration and EC. This result is interesting because non-linear temperature dependence of bulk EC is observed at high temperature ranges [*Waxman and Thomas, 1974*], and predicted by petrophysical models [*Revil et al., 1998; Waxman and Thomas, 1974*].

[9] In order to understand if a petrophysical model could predict these results and be employed for general use in future studies, we adopt the model presented by *Revil et al.* [1998, equation 10]. This model is chosen because the effective medium theory has a stronger theoretical foundation than those based on parallel resistors, and this model accounts for the differential movement of anions and cations

due to the negative surface charge on the mineral grains. The model uses linear temperature relationships for the fluid EC (σ^f) and the surface ionic mobility (B) which is directly proportional to the surface conductivity.

$$\sigma^f = \sigma^{f25} [m^f (T - 25) + 1] \quad (3a)$$

$$B = B^{25} [m^s (T - 25) + 1] \quad (3b)$$

Revil et al. [1998] calibrated the model using studies of the electrical conductivity of shaly sandstone cores as a function of temperature and fluid conductivity. The temperature range of these experiments was 25–200°C. The calibrated values are $m^f = 0.023$ and $m^s = 0.040$. However with these parameters, the model predicts a nonlinear bulk EC response that has a greater change in response to temperature than that of the data observed in our study.

[10] An exponential function based on Arrhenius's equation (equation 1) has been used in previous studies to describe the EC temperature relationship for fluid, surface and bulk EC [*Llera et al., 1990; Roberts, 2002; Waxman and Thomas, 1974; Ledo and Jones, 2005; Nover, 2005*]. If the exponential equation is a valid description, then a linear approximation calibrated over one temperature range will not be applicable to another. *Hayashi* [2004] found the linear EC temperature relationship (equation 2) for water over the 0–25°C range fit his data with a mean slope of $m = 0.0187$, whereas *Revil et al.* [1998] found $m^f = 0.023$ over the 25–200°C range. It appears that a linear model calibrated over the temperature range of 25–200°C for well-logging applications does not necessarily fit the data collected over the 0–25°C range for near surface monitoring applications. We would expect this same logic to apply to the temperature dependence of the surface EC. We fit the model presented in *Revil et al.* [1998] to our data using the $m^f = 0.0187$ value from *Hayashi* [2004]. This procedure returns m^s values ranging from 0.016 to 0.020 with a mean of 0.018 for the 8 laboratory data sets. The model by *Revil et al.* [1998, equation 10], fits our data quite well if we use low temperature range parameters of $m^s = 0.018$ and $m^f = 0.0187$ [*Hayashi, 2004*], and $B^{25} = 0.51 \times 10^{-8} \text{ m}^2 \text{ s}^{-1} \text{ V}^{-1}$ [*Hardwick, 1987*] (Figure 1b). The ionic mobility value, B^{25} , assumes a sodium counter ion.

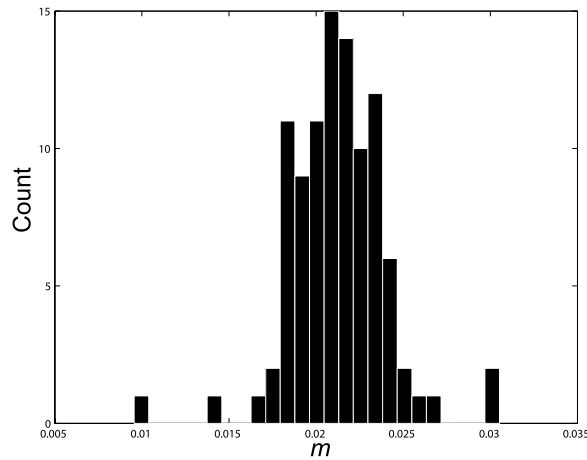


Figure 2. Histogram of extracted slopes from the analysis of the *Scott and Kay* [1988] study. This distribution has a mean of 0.021 and a standard deviation of 0.003.

[11] The analysis leads to two observations. First, exponential temperature relationships within the petrophysical model would provide better results over a larger temperature range. Second, the slopes of the linear approximations for the temperature dependence of surface and fluid conductivity at low temperature are similar, so the single linear relationship for the bulk conductivity that we observed in our laboratory data over a 0–25°C temperature range is consistent with the theoretical models.

[12] Our laboratory experiments yielded a consistent value of $m = 0.0183$ for the slope of the linear model, equation (2), relating bulk EC and temperature. In a study of EC of soils and sediments, *Scott and Kay* [1988] examined the temperature dependence of 91 soil samples from 12 field sites across Canada with variable geologic settings and depths of 0.5 to 10 m. We extracted the data from the 0 to 25°C temperature range and observed that the temperature-EC relationships followed an approximately linear trend. The slope of each 0 to 25°C data set was determined by least squares. The distribution of the derived slopes or m values is shown in Figure 2. This distribution has a mean of 0.021 and a standard deviation of 0.003. Our results are within one standard deviation of the mean. In comparison to our laboratory experiments the procedure used in the *Scott and Kay* [1988] study was less controlled in terms of saturation, packing and loading of the cell. The spread of m values from this study may be influenced by the material type, and sample saturation. Moreover, several of the datasets contain only three points so the resulting linear fits would be affected by experimental error. In spite of these issues, the distribution of fitted slopes in Figure 2 is narrow. Thus, these values can be used to account for the temperature dependence of a variety of near surface materials over the 0 to 25°C temperature range when an experiment like the one used in this study is not conducted.

[13] Although the fluid conductivity slope ($m^f = 0.023$) reported by *Revil et al.* [1998] is similar to the slopes derived in this study, the surface conductivity slope ($m_s = 0.040$) is not and predictions of nonlinear bulk EC temperature relationships are not observed. This supports our modification of the model parameters to low temperature

equivalents, and the use of a linear bulk EC temperature relationship over the 0 to 25°C temperature range.

4. Field Study

[14] Time lapse three dimensional ERI monitoring of a salt plume was conducted over the same site where the core samples for the temperature study were taken. Ten parallel lines were separated by 4 meters. Each line had 56 electrodes separated by 2 m. Lines were run with dipole-dipole configurations to a maximum n-spacing of 6. The ten lines of data were combined and jointly inverted with RES3DINV [*Loke and Barker, 1996*].

[15] The site is being remediated using tile drains installed at 2 m depth, and the goal of the time-lapse survey is to image the remediation and natural movement of the plume. The water table was measured at 2.3 m depth in a piezometer for the October 2005 survey and 2.6 m for May 2006. Data from two tensiometer nest installations and a soil water characteristic curve for a silty clay were used to estimate the saturation. Estimated saturation varied from 0.88 to 0.95 in the upper 0.5 m during each survey with similar magnitude variations between the survey periods. The estimated depth of the capillary fringe remained at 1 m depth. Temperature was recorded at the time of the surveys using two thermocouple installations completed to six meters and in piezometers below the water table. Figure 3 shows the temperature measurements recorded at the field station during the October 2005 and May 2006 surveys. Temperature was recorded at a variety of times and locations, giving an indication of the spatial and temporal variability of the subsurface temperature distribution during the survey collection period. This gives us a measure of the uncertainty in any temperature compensation calculation applied over the survey area. For example the variation of approximately 3.5°C in the upper meter during the May 2006 survey leads to maximum and minimum corrections that differ by 6.5%. We can see consistent trends showing the seasonal temperature variations penetrating the subsurface, with the temperatures stabilizing at around 6°C at nine meters depth.

[16] In order to remove the temperature effect from the time-lapse images we use the linear temperature dependence

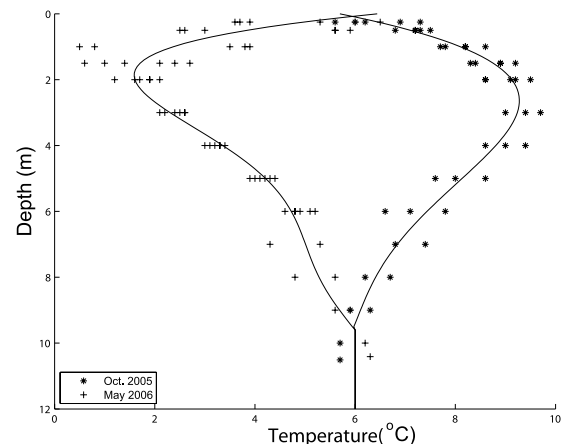


Figure 3. In situ temperature profiles from May 2006 and October 2005 survey times and best fit polynomials.

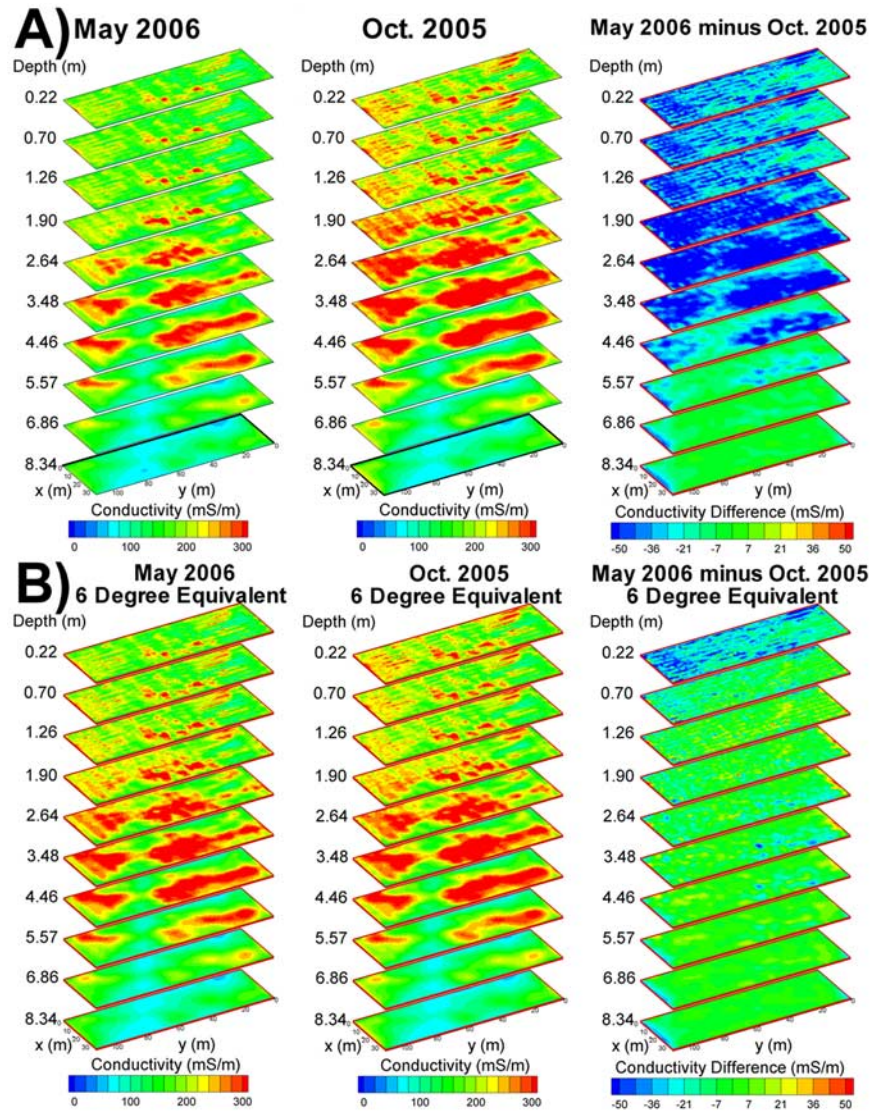


Figure 4. ERI inversion results from October 2005, May 2006, and the difference between them. (a) No temperature compensation. (b) 6°C equivalent images.

model to change the EC to a standard temperature equivalent before we make comparisons between images. The standard temperature we chose for our survey was 6°C to minimize the magnitude of the temperature compensation. We applied the relevant temperature profile shown by the lines in Figure 3 to each of the surveys. Some care has to be taken as all of the linear models use 25°C as the reference temperature, and the slope m is dependant on the reference temperature. In order to convert our data to a 6°C equivalent and to maintain the 25°C convention, we manipulate equation (2) to:

$$\sigma_{std} = \left[\frac{m(T_{std} - 25) + 1}{m(T_i - 25) + 1} \right] \sigma_i \quad (4)$$

where T_{std} and σ_{std} are the standard temperature and EC, T_i and σ_i are the in situ temperature and EC (i.e., taken from the temperature profile in Figure 3 and the resistivity inversion), and m is the slope calculated using the 25°C convention.

[17] Figure 4a shows the ERI inversion results that reflect in situ resistivity values and the May 2006 minus October 2005 difference. A negative difference dominates the upper 4 meters. Figure 4b shows the images after using equation (4) and the temperature profiles in Figure 4 to produce the 6°C equivalent images. The majority of the negative change in the May 2006 minus October 2005 no longer exists in the 6°C equivalent difference image. By removing the temperature effects from the difference image our interpretation of the images is altered from large scale seasonal solute movement and removal by the drain system to subtle effects due to saturation changes in the upper 50 cm, possible solute redistribution, and noise.

5. Conclusions

[18] Temperature dependence of EC in glacial till samples over the temperature range 0 to 25°C is not well described with petrophysical models that have been calibrated over 25–200°C. This discrepancy can be reconciled

by using an exponential relationship based on Arrhenius's equation or linear approximations specific to the temperature range of interest. Linear approximations for the surface and the fluid EC temperature dependence in this lower temperature range produce similar values for their slope, so a single linear approximation for the temperature dependence of the bulk EC describes observed data well. In this study and that of *Scott and Kay* [1988] using a variety near surface materials, the slope of the low temperature linear model is quite consistent. At least for Canadian sites, a value between 0.018 and 0.022 can be used if no other information is available.

[19] Neglecting temperature variations when using resistivity to track the movement of solute or soil moisture can lead to errors in interpretation of the geophysical results. Accounting for temperature variations is especially important when attempting quantitative estimates of concentration or moisture content from resistivity data or when comparing long-term time-lapse data images. Only by converting all images to a standard temperature equivalent can the results be compared to isolate solute movement and saturation changes. Many studies have tried to convert ERI images to solute concentration maps; however, if this is to be meaningful, then temperature variations within the image must be accounted for. Consequently, auxiliary data, such as that derived from the installation of temperature sensors, should be an integral component of any time-lapse survey or any survey seeking quantitative estimates of pore fluid concentration or variations in moisture content.

[20] **Acknowledgments.** The authors wish to thank the Environmental Research Advisory Council, Environment Canada (Program for Energy Research and Development), and the Natural Science and Engineering Research Council of Canada (NSERC) for funding. We also wish to thank Imperial Oil Resources for logistical and in-kind support and the Alberta Ingenuity Fund and NSERC for support of the first author.

References

- Barker, R., and J. Moore (1998), The application of time-lapse electrical tomography in groundwater studies, *Leading Edge*, 17, 1454–1458.
- Binley, A., P. Winship, L. J. West, M. Pokar, and R. Middleton (2002), Seasonal variation of moisture content in unsaturated sandstone inferred from borehole radar and resistivity profiles, *J. Hydrol.*, 267(3–4), 160–172.
- Bussian, A. E. (1983), Electrical conductance in a porous medium, *Geophysics*, 48(9), 1258–1268.
- Daily, W., A. Ramirez, D. LaBrecque, and J. Nitao (1992), Electrical resistivity tomography of vadose water movement, *Water Resour. Res.*, 28(5), 1429–1442.
- French, H., and A. Binley (2004), Snowmelt infiltration; monitoring temporal and spatial variability using time-lapse electrical resistivity, *J. Hydrol.*, 297(1–4), 174–186.
- Hardwick, A. (1987), The effect of brine composition on excess conductivity in shaly sands, paper presented at 28th Annual Logging Symposium, Soc. of Petrophys. and Well Log Anal., London.
- Hauck, C. (2002), Frozen ground monitoring using DC resistivity tomography, *Geophys. Res. Lett.*, 29(21), 2016, doi:10.1029/2002GL014995.
- Hayashi, M. (2004), Temperature-electrical conductivity relation of water for environmental monitoring and geophysical data inversion, *Environ. Monit. Assess.*, 96, 119–128.
- Kemma, A., J. Vanderborght, B. Kulesa, and H. Vereecken (2002), Imaging and characterisation of subsurface solute transport using electrical resistivity tomography (ERT) and equivalent transport models, *J. Hydrol.*, 267, 125–146.
- Ledo, J., and A. G. Jones (2005), Upper mantle temperature determined from combining mineral composition, electrical conductivity laboratory studies and magnetotelluric field observations: Application to the intermontane belt, Northern Canadian Cordillera, *Earth Planet. Sci. Lett.*, 236(1–2), 258–268.
- Llera, F. J., M. Sato, K. Nakatsuka, and H. Yokoyama (1990), Temperature dependence of the electrical resistivity of water-saturated rocks, *Geophysics*, 55(5), 576–585.
- Loke, M. H., and R. D. Barker (1996), Practical techniques for 3D resistivity surveys and data inversion, *Geophys. Prospect.*, 44(3), 499–523.
- Nover, G. (2005), Electrical properties of crustal and mantle rocks: A review of laboratory measurements and their explanation, *Surv. Geophys.*, 26(5), 593–651.
- Rein, A., R. Hoffmann, and P. Dietrich (2004), Influence of natural time-dependent variations of electrical conductivity on DC resistivity measurements, *J. Hydrol.*, 285(1–4), 215–232.
- Revil, A., L. M. Cathles III, S. Losh, and J. A. Nunn (1998), Electrical conductivity in shaly sands with geophysical applications, *J. Geophys. Res.*, 103(B10), 23,925–23,936.
- Roberts, J. J. (2002), Electrical properties of microporous rock as a function of saturation and temperature, *J. Appl. Phys.*, 91(3), 1687–1694.
- Scott, W. J., and A. E. Kay (1988), Earth resistivities of Canadian soils, research report, Can. Electr. Assoc., Montréal, Que., Canada.
- Sen, P. N., and P. A. Goode (1992), Influence of temperature on electrical conductivity on shaly sands, *Geophysics*, 57(1), 89–96.
- Slater, L. D., and S. K. Sandberg (2000), Resistivity and induced polarization monitoring of salt transport under natural hydraulic gradients, *Geophysics*, 65(2), 408–420.
- Waxman, M. H., and L. M. J. Smits (1968), Electrical conductivities in oil-bearing shaly sands, *Soc. Petr. Eng. J.*, 8(2), 107–122.
- Waxman, M. H., and E. C. Thomas (1974), Electrical conductivities in shaly sands: I. The relation between hydrocarbon saturation and resistivity index; II. The temperature coefficient of electrical conductivity, *J. Pet. Technol.*, 26(2), 213–225.
- Wong, R. C. K., L. R. Bentley, A. W. Ndegwa, A. Chu, M. Gharibi, and S. R. D. Lunn (2004), Biodegradation of monoethanolamine in soil monitored by electrical conductivity measurement: An observational approach, *Can. Geotech. J.*, 41, 1026–1037.

L. R. Bentley, M. Gharibi, K. Hayley, and M. Nightingale, Department of Geoscience, University of Calgary, 2500 University Drive, Northwest, Calgary, AB, Canada T2N 1N4. (khhayley@ucalgary.ca)